
Towards Personalized Federated Learning via Heterogeneous Model Reassembly (Supplementary Materials)

Anonymous Author(s)

Affiliation

Address

email

1 In this supplementary materials file, we provide additional content for the main manuscript due to the
2 page limit and requirements.

3 1 Pseudo-code of pFedHR

4 Algorithm 1 shows the pseudo-code of the proposed pFedHR model, which contains two main
5 updates: the server update (lines 3-11) and the client update (lines 12 - 17). The details of reassembly
6 candidate generation can be found in the main manuscript (Algorithm 1 on Page 5).

Algorithm 1: Algorithm Flow of pFedHR.

Input: Local data $\mathcal{D}_1, \mathcal{D}_2, \dots, \mathcal{D}_N$, the number of active clients B , communication rounds T , the
number of local training epochs E_c , the number of fine-tuning epochs at the server E_s ,
cluster number K .

```
1 for each communication round  $t = 1, 2, \dots, T$  do
2   Randomly sample  $B$  active clients and their model parameters are denoted as
    $\{\mathbf{w}_t^1, \mathbf{w}_t^2, \dots, \mathbf{w}_t^B\}$ ;
3   Server Update
4     for each  $n \in [1, \dots, B]$  do
5       Conduct layer-wise ecomposition on  $\mathbf{w}_t^n = [(\mathbf{L}_{t,1}^n, O_1^n), \dots, (\mathbf{L}_{t,H}^n, O_E^n)]$ ;
6     end
7     Conduct function-driven layer grouping with Eq. (4) to obtain  $\{\mathcal{G}_t^1, \mathcal{G}_t^2, \dots, \mathcal{G}_t^K\}$ ;
8     Conduct reassembly candidate generation to obtain  $\{\mathbf{c}_t^1, \dots, \mathbf{c}_t^M\}$  following
        $\mathcal{R}_1, \mathcal{R}_2, \mathcal{R}_3$ , and  $\mathcal{R}_4$ ;
9     Conduct layer stitching on the generated candidates;
10    Conduct similarity calculation on pairs of models with Eq. (5);
11    Distribute the personalized models back to the clients accordingly.
12  Client Update
13    for each  $n \in [1, \dots, B]$  do
14      for each local epoch  $e$  from 1 to  $E_c$  do
15        Update  $\mathbf{w}_t^n$  with Eq. (6);
16      end
17    end
18  Upload  $B$  models  $\{\mathbf{w}_t^1, \mathbf{w}_t^2, \dots, \mathbf{w}_t^B\}$  back to the server;
19 end
```

7 2 Implementation Details

8 The proposed pFedHR is implemented in Pytorch 2.0.1 and runs on NVIDIA A100 with CUDA
9 version 12.0 on a Ubuntu 20.04.6 LTS server. The hyperparameter λ in Eq. (6) is 0.2. We use Adam
10 as the optimizer. The learning rate of the local client learning and the server fine-tuning learning rate
11 are both equal to 0.001.

12 2.1 Model Details

13 In our experiments, we have 4 CNN models with different complexity. The details are shown as
14 follows. In each convolutional NN sequential block, there are 1 convolutional layer, a max pooling
15 layer, and a ReLU function.

16 **M1:** $Cov1:\{Conv2d (kernel\ size = 5) \rightarrow ReLU \rightarrow MaxPool2D (kernel\ size = 2, stride = 2)\}$
17 $\rightarrow Cov2:\{Conv2d (kernel\ size = 5) \rightarrow ReLU \rightarrow MaxPool2D (kernel\ size = 2, stride = 2)\} \rightarrow$
18 $FC1:\{Linear \rightarrow ReLU\} \rightarrow Dropout \rightarrow FC2:Linear.$

19 **M2:** $Cov1:\{Conv2d (kernel\ size = 5) \rightarrow ReLU \rightarrow MaxPool2D (kernel\ size = 2, stride = 2)\}$
20 $\rightarrow Cov2:\{Conv2d (kernel\ size = 5) \rightarrow ReLU \rightarrow MaxPool2D (kernel\ size = 2, stride = 2)\} \rightarrow$
21 $Cov3:\{Conv2d (kernel\ size = 5) \rightarrow ReLU\} \rightarrow FC1:\{Linear \rightarrow ReLU\} \rightarrow Dropout \rightarrow FC2:Linear.$

22 **M3:** $Cov1:\{Conv2d (kernel\ size = 5) \rightarrow ReLU \rightarrow MaxPool2D (kernel\ size = 2, stride = 2)\}$
23 $\rightarrow Cov2:\{Conv2d (kernel\ size = 5) \rightarrow ReLU \rightarrow MaxPool2D (kernel\ size = 2, stride = 2)\} \rightarrow$
24 $Cov3:\{Conv2d (kernel\ size = 5) \rightarrow ReLU\} \rightarrow Cov4:\{Conv2d (kernel\ size = 5) \rightarrow ReLU \rightarrow MaxPool2D$
25 $(kernel\ size = 2, stride = 2)\} \rightarrow Cov4:\{Conv2d (kernel\ size = 5) \rightarrow ReLU\} \rightarrow FC1:\{Linear \rightarrow ReLU$
26 $\rightarrow Dropout\} \rightarrow FC2:\{Linear \rightarrow ReLU\} \rightarrow FC3:\{Linear \rightarrow ReLU\} \rightarrow FC4:Linear.$

27 **M4:** $Cov1:\{Conv2d (kernel\ size = 5) \rightarrow BatchNorm2d \rightarrow ReLU\} \rightarrow Cov2:\{Conv2d (kernel\ size =$
28 $3) \rightarrow ReLU \rightarrow MaxPool2D (kernel\ size = 2, stride = 2)\} \rightarrow Cov3:\{Conv2d (kernel\ size = 3) \rightarrow$
29 $BatchNorm2d \rightarrow ReLU\} \rightarrow Cov4:\{Conv2d (kernel\ size = 5) \rightarrow ReLU \rightarrow MaxPool2D (kernel\ size$
30 $= 2, stride = 2) \rightarrow Dropout\} \rightarrow Cov5:\{Conv2d (kernel\ size = 3) \rightarrow BatchNorm2d \rightarrow ReLU\} \rightarrow$
31 $Cov6:\{Conv2d (kernel\ size = 3) \rightarrow ReLU \rightarrow MaxPool2D (kernel\ size = 2, stride = 2)\} \rightarrow FC1:\{Linear$
32 $\rightarrow ReLU \rightarrow Dropout\} \rightarrow FC2:\{Linear \rightarrow ReLU\} \rightarrow FC3:\{Linear \rightarrow ReLU\} \rightarrow FC4:Linear.$

33 2.2 Details of Rule \mathcal{R}_2 (Operation Order)

34 We introduce the rule \mathcal{R}_2 (operation order) in Line 11 of the algorithm in the main manuscript. We
35 follow existing work [1–5] to define the following rules:

- 36 1. A CNN typically has convolutional layers, pooling layers, and fully connected layers, which
37 requires the generated candidate to have these functional layers.
- 38 2. The typical operation order is convolution layers \rightarrow ReLU layers \rightarrow pooling layers \rightarrow fully
39 connected layers.

40 2.3 Public Data Sensitivity Analysis

41 2.3.1 Layer Stitching Study

42 One of our major contributions is to develop a new layer stitching strategy to reduce the adverse
43 impacts of introducing public data, even with different distributions from the client data. Our proposed
44 strategy includes two aspects: (1) using a simple layer to stitch layers and (2) reducing the number
45 of finetuning epochs. To validate the correctness of these assumptions, we conduct the following
46 experiments on SVHN with 12 clients, where both client data and **labeled** public data are extracted
47 from SVHN.

48 **Stitching Layer Numbers.** In this experiment, we add the complexity of layers for stitching. In
49 our model design, we only use $ReLU(\mathbf{W}^T \mathbf{X} + \mathbf{b})$. Now, we increase the number of linear layers
50 from 1 to 2 to 3. The results are depicted in Figure 1. We can observe that under both IID and
51 Non-IID settings, the performance will decrease with the increase of the complexity of the stitching
52 layers. These results demonstrate our assumption that more complex stitching layers will introduce
53 more information about public data but reduce the personalized information of each client model
54 maintained. Thus, using a simple layer to stitch layers is a reasonable choice.

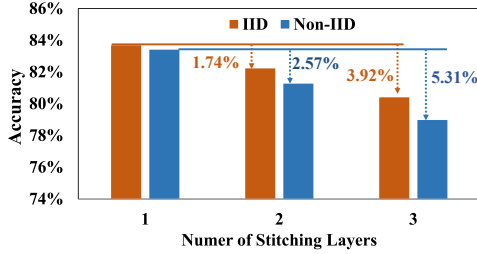


Figure 1: Stitching layer number study.

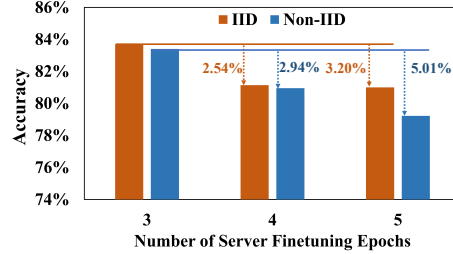


Figure 2: Server finetuning number study.

55 **Stitched Model Finetuning Numbers.** We further explore the influence of the number of finetuning
 56 epochs on the stitched model. The results are shown in Figure 2. We can observe that increasing
 57 the number of finetuning epochs can also introduce more public data information and reduce model
 58 performance. Thus, setting a small number of finetuning epochs benefits keeping the model’s
 59 performance.

60 2.3.2 Experiment results with Different Numbers of Clusters

61 In our model design, we need to group functional layers into K groups by optimizing Eq. (4). Where
 62 K is a predefined hyperparameter. In this experiment, we aim to investigate the performance influence
 63 with regard to K . In particular, we conduct the experiments on the SVHN dataset with 12 local
 64 clients, and the public data are also the SVHN data.

65 Figure 3 shows the results on both IID and Non-IID settings with labeled and unlabeled public data.
 66 X -axis represents the number of clusters, and Y -axis denotes the accuracy values. We can observe
 67 that with the increase of K , the performance will also increase. However, in the experiments, we do
 68 not recommend setting a large K since a trade-off balance exists between K and M , where M is the
 69 number of candidates automatically generated by Algorithm 1 in the main manuscript. If K is large,
 70 then M will be small due to Rule \mathcal{R}_4 . In other words, a larger K may make the empty \mathcal{C}_t returned by
 71 Algorithm 1 in the main manuscript.

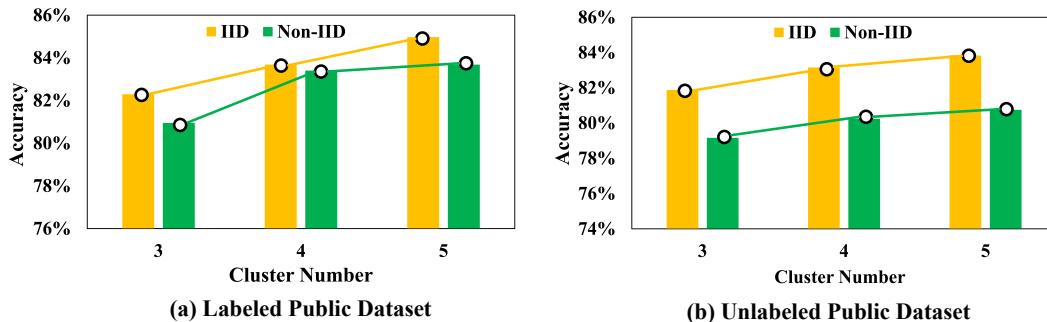


Figure 3: Results on different number of clusters K ’s.

72 2.3.3 Experiment Results of Public Data Sensitivity on SVHN with 100 Clients

73 Figure 4 shows the experimental results with 100 clients. The clients hold the SVHN data, and we
 74 alternatively change the (labeled and unlabeled) public data and report the results for both IID and
 75 Non-IID settings. We can observe the same results as those on the 12 clients (Figure 1 in the main
 76 manuscript). All approaches can achieve the best performance when using SVNH as the public data.
 77 Although using other public data, the performance of all approaches drops, the performance change
 78 of the proposed pFedHR is lowest. Besides, even using other public data, pFedHR can achieve
 79 comparable or better performance to baselines. For example, in Figure 4(b), when pFedHR uses the
 80 MNIST as the public data, its performance is comparable to FedMD and better than FedGH using
 81 SVHN as the public data. These results confirm that the proposed pFedHR can handle the public
 82 data sensitivity issue.

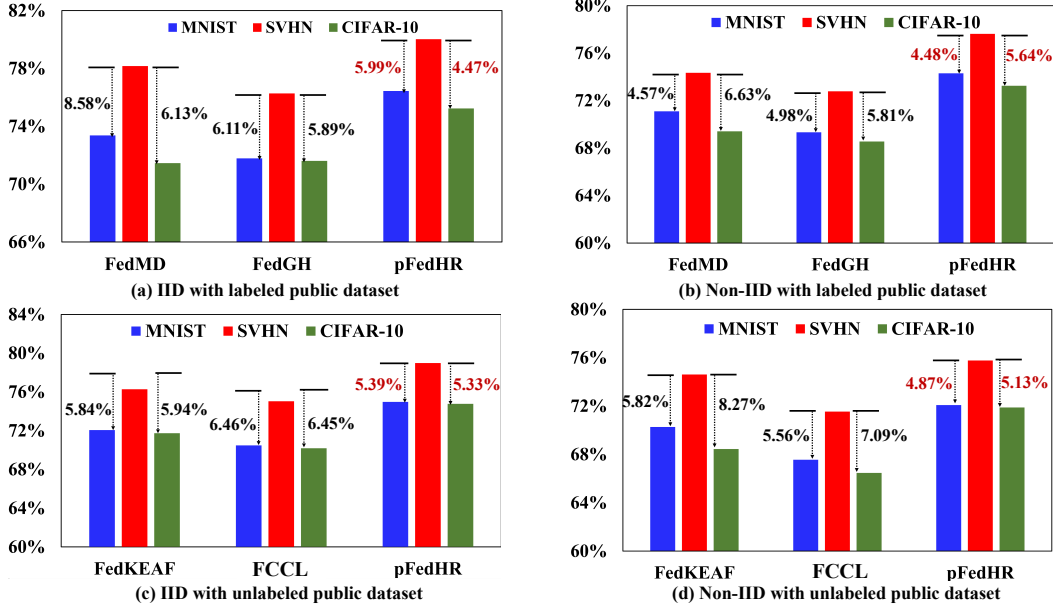


Figure 4: Results with 100 clients.

83 **2.3.4 Experiment Results of Public Data Sensitivity on CIFAR-10 with 12 Clients**

84 We also validate the public data sensitivity on CIFAR-10, where clients hold data from CIFAR-10,
 85 and we alternatively change the public data. The results are shown in Figures 5 and 6. We have the
 86 same observations as we discussed before. Using public data with different distributions makes the
 87 performance drop, but the proposed pFedHR has the smallest drop ratio.

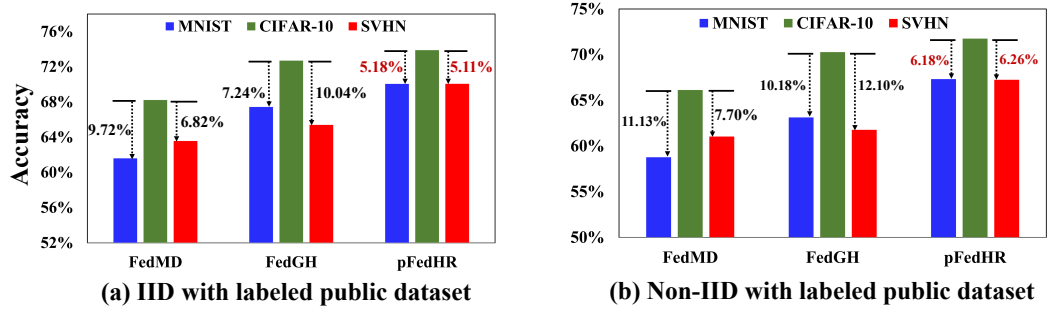


Figure 5: Results with CIFAR-10 private dataset and labeled public datasets.

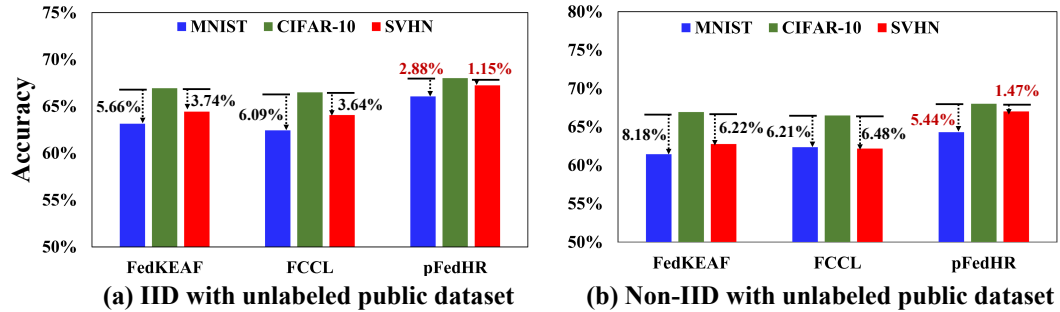


Figure 6: Results with CIFAR-10 private dataset and unlabeled public datasets.

88 3 Limitation

89 All the experimental results demonstrate the effectiveness of the proposed pFedHR. However,
90 pFedHR still have the following limitations:

- 91 1. In our experiments, we use four different CNN-based models and randomly send them
92 to clients. The reason for using these simple models is that they can save computational
93 resources. In our model design, we will calculate the CKA score between any pair of layers.
94 In other words, if the local model is very deep (with multiple layers), the computational
95 complexity will be very high.
- 96 2. In real-world applications, the client models may be more complicated. To deploy the
97 proposed pFedHR in a real environment, we need to slightly modify the layer-wise decom-
98 position and use block-wise decomposition as [6] and redefine the rules used for generating
99 candidates accordingly.
- 100 3. In our experiments, we only test the designed model on the image datasets. In real-world
101 applications, multiple types of data may be stored in each client. How to handle other types
102 of data with heterogeneous model reassembly is one of our major future works.

103 4 Broader Impacts

104 The proposed pFedHR addresses the practical challenge of model heterogeneity in federated learning.
105 By introducing heterogeneous model reassembly and personalized federated learning, this research
106 contributes to the advancement of federated learning techniques, potentially improving the efficiency
107 and effectiveness of collaborative machine learning in distributed systems.

108 The pFedHR framework automatically generates informative and diverse personalized candidates
109 with minimal human intervention. This has the potential to reduce the burden on human experts
110 and practitioners, making the process of model personalization more efficient and scalable. It opens
111 up possibilities for deploying federated learning systems in real-world scenarios where manual
112 customization is impractical or time-consuming.

113 The proposed heterogeneous model reassembly technique in pFedHR try to mitigate the adverse
114 impact caused by using public data with different distributions from the client data. This can be
115 beneficial in scenarios where privacy concerns limit the availability of extensive client data, such as
116 healthcare, enabling the utilization of publicly available data while maintaining a certain level of
117 model performance. It promotes the ethical and responsible use of data and encourages collaboration
118 between organizations and researchers in a privacy-preserving manner.

119 References

- 120 [1] Alex Krizhevsky, Ilya Sutskever, and Geoffrey E Hinton. Imagenet classification with deep
121 convolutional neural networks. *Communications of the ACM*, 60(6):84–90, 2017.
- 122 [2] Karen Simonyan and Andrew Zisserman. Very deep convolutional networks for large-scale
123 image recognition. *arXiv preprint arXiv:1409.1556*, 2014.
- 124 [3] Kaiming He, Xiangyu Zhang, Shaoqing Ren, and Jian Sun. Deep residual learning for image
125 recognition. In *Proceedings of the IEEE conference on computer vision and pattern recognition*,
126 pages 770–778, 2016.
- 127 [4] Christian Szegedy, Wei Liu, Yangqing Jia, Pierre Sermanet, Scott Reed, Dragomir Anguelov,
128 Dumitru Erhan, Vincent Vanhoucke, and Andrew Rabinovich. Going deeper with convolutions.
129 In *Proceedings of the IEEE conference on computer vision and pattern recognition*, pages 1–9,
130 2015.
- 131 [5] Gao Huang, Zhuang Liu, Laurens Van Der Maaten, and Kilian Q Weinberger. Densely connected
132 convolutional networks. In *Proceedings of the IEEE conference on computer vision and pattern
133 recognition*, pages 4700–4708, 2017.
- 134 [6] Xingyi Yang, Daquan Zhou, Songhua Liu, Jingwen Ye, and Xinchao Wang. Deep model
135 reassembly. *Advances in neural information processing systems*, 35:25739–25753, 2022.